proton transfer and the chlorine abstraction require the surmounting of small barriers. A comparison of the energy profiles shown in Figures 1 and 2 makes it clear that the three-step mechanism offers a much faster pathway.

To our knowledge, this alternative reaction mechanism has not been discussed before. However, the single steps can easily be interpreted: the Lewis adduct $H_3N \cdot BCl_3$, which contains a fourfold coordinated nitrogen atom, is a Brønsted acid in liquid NH_3. It loses a proton, which immediately forms an ammonium ion with one of the solvent molecules. The resulting anion is unstable and eliminates a chloride anion to form the neutral and stable BCl_2NH_2.

Calculation Methods

For all static calculations, a valence-triple-zeta basis set with a polarization function (TZVP) was used. The corresponding auxiliary basis sets were used for the resolution of identity (RI) approximation of the two-electron integrals.[7–9] The structures and energies were determined by RI-approximated second-order Møller–Plesset perturbation theory (RI-MP2)[10] by employing the TURBOMOLE 5.1[11, 12] and ef.x[13] programs. All simulations were performed by using the Car–Parrinello Molecular Dynamics code, Version 3.0 h.[14] For these calculations, we employed the Becke(88) exchange and Lee–Yang–Parr correlation functionals (BLYP).[15, 16] The reliability of various nonhybrid density functionals (SVWN, BLYP, HCTH, PBE) was tested by comparing the relative energies of stationary points on the potential energy hypersurface of the gas-phase reaction with results from previous RI-MP2 calculations.[3] BLYP showed the best performance of these functionals: the relative energies of the transition state and the products with respect to the reactants agree very well (± 1 kJ mol^{-1}). On the other hand, the adduct formation energy is underestimated by 44 kJ mol^{-1}. An error of this size is typical for the description of dative bonds with DFT methods and cannot easily be remedied.[17] The valence electrons were described with a plane-wave basis set with an energy cutoff of 60 Ry ($\approx 131 \times 10^{-18}$ J). An extension of the energy cutoff to 70 Ry ($\approx 153 \times 10^{-18}$ J) has no significant effect on structure and energy. Troullier–Martins pseudopotentials were employed for the representation of the inner electrons.[18] The simulations at the microcanonical (f(N,V,E)) ensemble were performed with time steps of 4 a.u. (0.0968 fs) and a fictitious electron mass of 400 a.u (3.64×10^{-28} kg). One BCl_3 and eleven NH_3 molecules were placed in a cubic box ((7.94 Å)^3). This corresponds to a density of ≈ 1 g cm^{-3}, comparable to the density of liquid BCl_3 at 286 K (1.4 g cm^{-3}) and the density of liquid ammonia at 240 K (0.7 g cm^{-3}). The energies of the arbitrarily chosen starting geometries were optimized (T = 0 K), that is, they constitute local minima on the potential hypersurface. The initial momenta of the ions were chosen according to a Maxwell–Boltzmann distribution. The delocalized molecular orbitals were transformed into localized Wannier functions to investigate the spatial localization of the electrons.[19, 20]

Received: April 19, 2001 [Z 16960]

[1] F. Meyer, R. Zappner, *Ber. Dtsch. Chem. Ges.* **1921**, *54*, 560.
[2] R. T. Paine, C. K. Narula, *Chem. Rev.* **1990**, *90*, 73.
[3] S. Reinhardt, M. Gastreich, C. M. Marian, *Phys. Chem. Chem. Phys.* **2000**, *2*, 955.
[4] R. Car, M. Parrinello, *Phys. Rev. Lett.* **1985**, *55*, 2471.
[5] R. Car, M. Parrinello, *Phys. Rev. Lett.* **1988**, *60*, 204.
[6] M. Parrinello, *Solid State Commun.* **1997**, *102*, 107.
[7] A. Schäfer, H. Horn, R. Ahlrichs, *J. Chem. Phys.* **1992**, *97*, 2571.
[8] F. Weigend, M. Häser, *Theor. Chem. Acc.* **1997**, 331.
[9] F. Weigend, M. Häser, H. Patzelt, R. Ahlrichs, *Chem. Phys. Lett.* **1998**, *294*, 143.
[10] C. Møller, M. S. Plesset, *Phys. Rev.* **1934**, *46*, 618.
[11] R. Ahlrichs, M. Bär, M. Häser, H. Horn, C. Kölmel, *Chem. Phys. Lett.* **1989**, *162*, 165.
[12] The Turbomole homepage can be found under http://www.chemie.uni-karlsruhe.de/PC/TheoChem.
[13] ef.x: S. Grimme, M. Gleichmann, M. Gastreich, C. M. Marian, Universität Bonn, **1996**.
[14] CPMD: J. Hutter, P. Ballone, M. Bernasconi, P. Focher, E. Fois, S. Goedecker, M. Parrinello, M. Tuckerman, Max-Planck-Institut für Festkörperforschung, Stuttgart, and IBM Research Division, Zürich, **1990–1996**.
[15] A. D. Becke, *Phys. Rev. A* **1988**, *38*, 3098.
[16] C. Lee, W. Yang, R. G. Parr, *Phys. Rev. B* **1988**, *37*, 785.
[17] R. Ahlrichs, F. Furche, S. Grimme, *Chem. Phys. Lett.* **2000**, *325*, 317.
[18] N. Troullier, J. L. Martins, *Phys. Rev. B* **1991**, *43*, 1993.
[19] P. L. Silvestrelli, N. Marzari, D. Vanderbilt, M. Parrinello, *Solid State Commun.* **1998**, *107*, 7.
[20] G. Berghold, C. Mundy, A. Romero, J. Hutter, M. Parrinello, *Phys. Rev. B* **2000**, *61*, 10040.

DNA-Directed Functionalization of Colloidal Gold with Proteins**

Christof M. Niemeyer* and Bülent Ceyhan

The utilization of nucleic acids and proteins as building blocks in the "bottom-up" self-assembly of nanoscale functional devices is of great current interest.[1] As an example, DNA has been applied to fabricate nanostructured molecular scaffolding and surface architectures,[2] and to selectively position proteins[3] and nanoclusters[4] on the nanometer scale. In earlier work, we reported the DNA-directed immobilization of proteins,[5, 6] which concerned the binding of single-stranded DNA-tagged immunoglobulins (IgG) or enzymes to surface-immobilized complementary capture oligonucleotides by means of the highly specific Watson–Crick base pairing. This method not only allows a surprisingly efficient and fully reversible adsorption of the proteins, but also it enables the simultaneous immobilization of many different DNA-tagged components in a single, site-selective process using a DNA microarray as a capture matrix. We here report on the DNA-directed immobilization of proteins at colloidal gold, as well as on applications of the resulting biofunctionalized nanoparticles in immunological detection methods.

To allow the modular functionalization of gold nanoparticles (Au-**1**) modified with oligonucleotide **1** (see Experimental Section), we chose the covalent DNA–streptavidin (STV) conjugate **4** as a molecular linker. **4** was obtained from the biotin-binding protein STV **3** and 5′-thiol-modified oligonucleotides **2**, using the heterobispecific amino/thiol-reactive

[*] Priv.-Doz. Dr. C. M. Niemeyer, Dipl.-Chem. B. Ceyhan
Universität Bremen, FB2-UFT
Biotechnologie und Molekulare Genetik
Leobener Strasse 28359 Bremen
Fax: (+49) 421-218-7578
E-mail: cmn@uni-bremen.de

[**] This work was supported by Deutsche Forschungsgemeinschaft and Fonds der Chemischen Industrie. We thank Prof. D. Blohm for helpful discussions and generous support.

cross-linker sulfosuccinimidyl-4-(maleimidomethyl)cyclohexane-1-carboxylate (sSMCC).[5] The oligonucleotide moiety in **4** expands the tetravalent binding capacity of the native STV for biotin by one highly specific binding site for complementary nucleic acids. Thus, **4a** can be used as a biomolecular adapter in the coupling of biotinylated antibodies with Au-**1**, which is modified with the complementary oligonucleotide (Scheme 1).

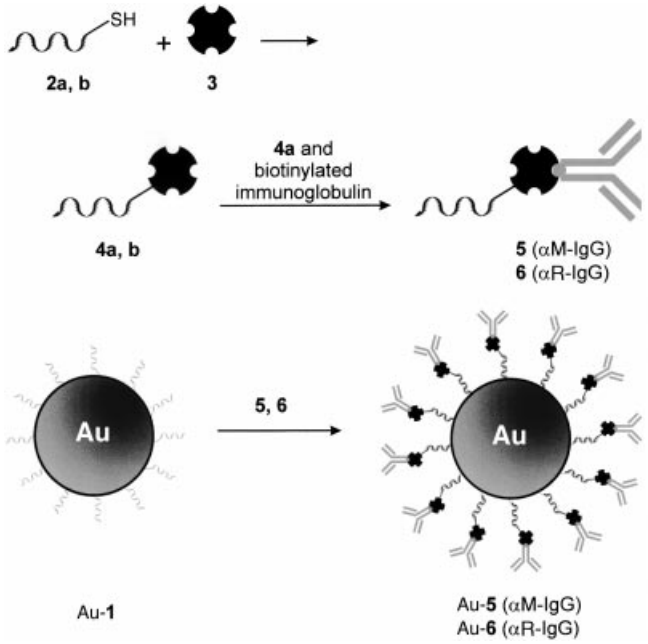

Scheme 1. DNA-directed immobilization of proteins at gold colloids using the covalent DNA – STV conjugates **4**, obtained from STV **3** and 5′-thiol-modified oligonucleotides **2a**, **b**. The oligonucleotide **2a** is complementary to the gold colloid bound oligomer **1**. The coupling of **4a** with biotinylated antibodies directed against mouse IgG (αM-IgG) or rabbit IgG (αR-IgG) leads to the DNA-tagged antibody conjugates **5** and **6**, respectively, which bind to Au-**1** by specific nucleic acid hybridization. Complementary DNA strands are drawn as helices. The 3′-ends are indicated by arrow heads.

To experimentally test our concept, we carried out gel electrophoretic measurements (Figure 1) using oligonucleotide **1** covered colloidal gold particles of a mean diameter of 34 nm (Au_{34}-**1**), which were incubated with 100 molar equivalents of the complementary DNA – STV hybrid **4a** at room temperature for 60 min. The comparison of the electrophoretic mobility of Au_{34}-**1** and STV-coated Au_{34}-**4** clearly indicated the coupling of the proteins at the gold particles (lanes 1 and 2, in Figure 1). The specificity of the protein coupling was demonstrated in lane 3, by using a control in which the noncomplementary DNA – STV hybrid **4b** was mixed with Au_{34}-**1**. To immobilize antibodies at the surface of the gold nanoparticles, STV conjugate **4a** was initially coupled with one molar equivalent of an antibody against the mouse IgG antigen (αM-IgG), and without any further purification, the resulting conjugate **5** was incubated with 1 mol% of Au_{34}-**1** at room temperature for 60 min. The electrophoretic mobility of anti-mouse IgG functionalized Au_{34}-**5** was less than that of the STV-modified Au_{34}-**4** (lanes 4

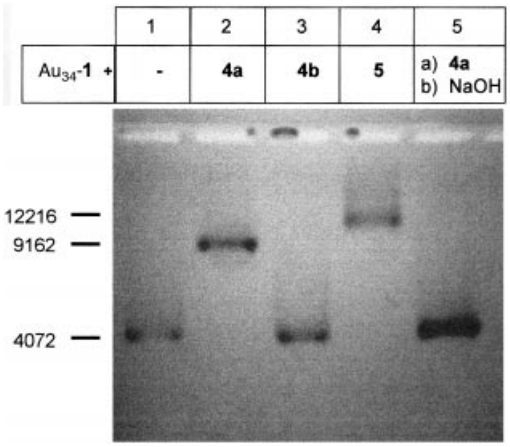

Figure 1. Electrophoretic analysis of the DNA-directed immobilization of proteins at gold nanoparticles. Shown is a grayscale representation of a nondenaturing 1.5% agarose gel (the bands are in fact reddish-purple because of the characteristic absorption of the colloidal gold). The bands indicate the mobility of Au_{34}-**1** (lane 1), Au_{34}-**1** coupled with the complementary DNA – STV hybrid **4a** (lane 2), Au_{34}-**1** mixed with the noncomplementary DNA – STV hybrid **4b** (lane 3), Au_{34}-**1** coupled with the complementary antibody conjugate **5** (lane 4), and Au_{34}-**1**, which was initially coupled with the complementary DNA – STV hybrid **4a** and subsequently treated with NaOH to remove the bound proteins (lane 5). The mobility of the DNA fragments of a DNA molecular-weight marker is given in base pairs.

and 2, in Figure 1), which indicates the successful binding of the DNA-tagged antibodies at the gold nanoparticles. Moreover, comparison of the lanes 1, 2, and 5 in Figure 1 indicates that the DNA-bound proteins can be removed from the particles by washing with NaOH and collection of the remaining Au_{34}-**1** by centrifugation. This reversibility of the protein adsorption not only illustrates the remarkable stability of DNA-coated gold nanoparticles, but it can also be utilized for their regeneration on the preparative scale.

The functionality of the antibody-modified nanoparticles **5** was evaluated in a sandwich immunoassay, in which various amounts of the model antigen mouse IgG were specifically immunosorbed through surface-immobilized capture antibodies (Scheme 2). The subsequent coupling Au_{34}-**5** to the antigen led after a short incubation period, to the formation of a characteristic reddish color at the surface, because of the immobilization of the colloidal gold. A silver development was carried out for signal amplification. The chemical reduction of silver ions, which is promoted by gold colloids, is a standard technique in histochemical analyses,[7] and it has recently been applied in the scanometric detection of nucleic acid hybridization,[8] as well as in the electrical detection of immuno reactions.[9] Here, the development of the silver layer was followed by spectrophotometry using a microplate reader, or else by imaging with a flatbed scanner (Figure 2). The signal intensities obtained depended on the amount of antigen present, which indicates that anti-mouse IgG functionalized Au_{34}-**5** allowed the specific detection of the complementary mouse antigen. Controls were carried out using anti-rabbit IgG functionalized Au_{34}-**6**, or else a mixture consisting of Au_{34}-**1** and anti-mouse IgG coupled with the noncomplementary STV conjugate **4b** instead of Au_{34}-**5**. No significant silver development was observed in these controls. The measure-

  1433-7851/01/4019-3686 $ 17.50+.50/0 *Angew. Chem. Int. Ed.* **2001**, *40*, No. 19

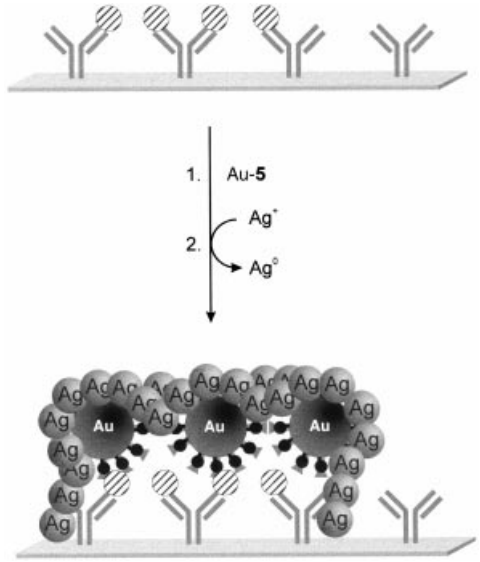

Scheme 2. Utilization of antibody/DNA-functionalized gold colloids as reagents in a sandwich immunoassay. The model antigen mouse IgG, (striped circles), is bound by surface-attached capture antibodies through specific immunosorption, and the antigen is labeled with anti-mouse functionalized Au-**5**. For signal generation, a silver development is carried out. The generation of silver is monitored spectrophotometrically or by imaging with a camera or a flatbed scanner.

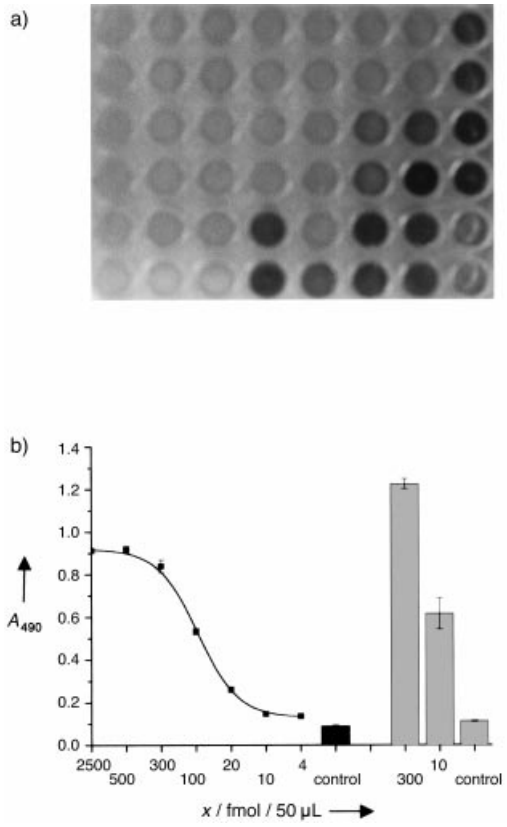

Figure 2. Utilization of the antibody functionalized nanoparticles Au_{34}-**5** and Au_{13}-**5** as reagents in a sandwich-immunoassay (see Scheme 2). a) Wells of a microplate with silver films developed to a varying extent; b) the absorbance at 490 nm of the silver film depended on the amount *x* of antigen present in the samples. The data points in the left side of the diagram were obtained for Au_{34}-**5**, the gray histograms represent signals obtained with Au_{13}-**5**. The controls were carried out with pure silver-development solution, applied in the absence of other reagents.

mentof a serial dilution indicated that less than 10 fmol of the antigen were detectable. Thus, the detection limit of this assay is similar to that of conventional enzyme-amplified immunoassays.[10]

Further experiments concerned the influences of the coupling ratio of Au_{34}-**1** and DNA-tagged antibody conjugate **5**. Maximum signal intensities were obtained at a relative stoichiometry of about 1:100 for Au_{34}-**1**:**5**, and a decrease in signal was obtained at the higher coupling ratio of 1:200. This is a result of the competition between Au_{34}-**1**-bound and unbound **5**, and correlates with earlier studies, which indicate that the hybridization efficiency of colloidal gold surfaces is about 6% of the total number of oligonucleotides attached.[11] Experiments currently in progress suggest that the optimization of reagents and reaction parameters will further enhance the detection limit of the immunoassay. For instance, the use of smaller 13 nm gold colloids, functionalized with anti-mouse IgG through a DNA bridge (Au_{13}-**5**), already allowed us to enhance the signal intensities in the sandwich immunoassay (Figure 2). These experiments also clearly indicate that the modular construction approach described here is fully applicable to the functionalization of other colloidal particles.

Herein we reported the convenient and efficient DNA-directed adsorption of proteins at colloidal gold. The biofunctionalized Au nanoparticles not only reveal extraordinary stability and regeneration properties, but they also possess the undisturbed, specific recognition capabilities of the colloid-bound proteins. In an initial application, the biometallic hybrid components were used as reagents in an immunoassay for the detection of proteins. Owing to the gold-particle promoted silver development, low amounts of antigen were detectable. Moreover, because of the lack of diffusion, the development of a silver layer can be used for the site-specific detection of surface-bound antigens.[12] Thus, the protein/DNA-modified gold colloids are particularly suited for the analysis of protein microarrays, which are increasingly applied in immunological diagnostics[13] and proteom research.[14] The biofunctionalized particles should also be suitable for surface-plasmon resonance detection.[15] Moreover, since the specificity of nucleic acid hybridization allows the simultaneous functionalization of various different DNA-coated Au colloids, particle-bound combinatorial DNA-arrays[16] might be transformed into corresponding protein arrays for parallel immunoassays. In addition to these bioanalytical applications, the approach described here has also implications for the development of nanostructured hybrid materials.[17, 18]

Experimental Section

Covalent DNA–STV conjugates **4a**,**b** were prepared from 5′-thiolated oligonucleotides (Interactiva, Ulm) and recombinant STV (IBA, Göttingen) in 10–15% yields using the heterobispecific cross-linker sSMCC (Pierce).[5] The nucleotide sequences of the STV-coupled oligomers were: 5′-Thiol-AGC GGA TAA CAA TTT CAC ACA GGA-3′ (**2a**), 5′-Thiol-CCG GGT ACC GAG CTC GAA TTC-3′ (**2b**), the sequence of the gold colloid bound oligomer **1** was: 5′-Thiol-TCC TGT GTG AAA TTG TTA TCC GCT-3′. The preparation of the DNA-coated gold nanoparticles Au-**1** was carried out as previously described using 15 nm and 40 nm colloids (ICN Biochemicals, Eschwege) with a diameter of 13.2 ± 0.6 (Au_{13}) or 34.2 ± 2.7 nm (Au_{34}),[19] as determined by transmission electron microscopy.

  1433-7851/01/4019-3687 $ 17.50+.50/0

To prepare the DNA – STV antibody conjugates **5**: a solution of **4a** (150 μL, 28 nM) in Tris-buffer (10 mM, pH 7.3), containing EDTA (1 mM), and 0.05 % Tween-20 (Tris – EDTA – Tween buffer solution, TETBS) were mixed with solution of biotinylated goat anti-mouse IgG (Sigma, Deisenhofen; 150 μL of a 28 nM) in TETBS, and the mixture was incubated for 10 min at room temperature (Tris = tris(hydroxymethyl)aminomethane, EDTA = ethylenediaminetetraacetic acid, Tween-20 = polyoxyethylenesorbitanmonolaurate). In a similar way, conjugate **6** was prepared from biotinylated goat anti-rabbit IgG (Sigma, Deisenhofen). To couple **5** or **6** with Au-**1**, 275 μL of the above solution were mixed with the same volume of a solution of Au_{34}-**1** (0.14 nM), or else, with the same volume of a solution of Au_{13}-**1** (1.16 nM), and the mixture was incubated for 1 h at room temperature.

To carry out the sandwich immunoassay, microplates were coated with a solution of goat anti-mouse IgG (Sigma, Deisenhofen; 50 μL, 20 nM), and subsequently blocked with milk powder to avoid nonspecific binding.[20] 50 μL of a solution containing varying amounts of the model antigen mouse IgG were added to each well of the microplate, and subsequent to incubation for 45 min, the plate was washed to remove unbound reagents. Coupling of Au-**5** was achieved by adding a solution of Au_{34}-**5** (50 μL, 0.07 nM), or else, a solution of Au_{13}-**5** (50 μL, 0.58 nM), and incubation for 45 min. Subsequent to washing, 50 μL of a silver enhancement kit (BioRad)[21] were added to the wells, and the development of silver was monitored spectrophotometrically at 490 nm or by imaging with a flatbed scanner.

Received: April 30, 2001 [Z17009]

[1] C. M. Niemeyer, *Curr. Opin. Chem. Biol.* **2000**, *4*, 609 – 618.
[2] N. C. Seeman, *Trends Biotechnol.* **1999**, *17*, 437 – 443.
[3] C. M. Niemeyer, *Chem. Eur J.* **2001**, *7*, 3188 – 3195.
[4] J. J. Storhoff, C. A. Mirkin, *Chem. Rev.* **1999**, *99*, 1849 – 1862.
[5] C. M. Niemeyer, T. Sano, C. L. Smith, C. R. Cantor, *Nucleic Acids Res.* **1994**, *22*, 5530 – 5539.
[6] C. M. Niemeyer, L. Boldt, B. Ceyhan, D. Blohm, *Anal. Biochem.* **1999**, *268*, 54 – 63.
[7] C. S. Holgate, P. Jackson, P. N. Cowen, C. C. Bird, *J. Histochem. Cytochem.* **1983**, *31*, 938 – 944.
[8] T. A. Taton, C. A. Mirkin, R. L. Letsinger, *Science* **2000**, *289*, 1757 – 1760.
[9] O. D. Velev, E. W. Kaler, *Langmuir* **1999**, *15*, 3693 – 3698.
[10] J. R. Crowther, *ELISA: Theory and Practice*, Humana Press, Totowa, New York, **1995**.
[11] Similar gold nanoparticles revealed a surface coverage of about 15 – 30 pmol DNA cm^{-2}, and about 6 % of this was accessible for intermolecular hybridization with complementary oligonucleotides: L. M. Demers, C. A. Mirkin, R. C. Mucic, R. A. Reynolds, R. L. Letsinger, R. Elghanian, G. Viswanadham, *Anal. Chem.* **2000**, *72*, 5535 – 5541. Thus, Au_{34}-**1** should contain about 1800 oligonucleotides per particle. The maximum binding capacity of Au_{34}-**1** of about 100 molar equivalents of **5** correllates with a hybridization efficiency of approximately 5.5 %.
[12] Preliminary results indicate that proteins, covalently bound to glass slides, can be specifically labeled with Au-**5**. The silver development leads to the formation of sharp spots which can be analyzed with a commercial flatbed scanner.
[13] R. M. de Wildt, C. R. Mundy, B. D. Gorick, I. M. Tomlinson, *Nat. Biotechnol.* **2000**, *18*, 989 – 994.
[14] G. MacBeath, S. L. Schreiber, *Science* **2000**, *289*, 1760 – 1763.
[15] L. He, M. D. Musick, S. R. Nicewarner, F. G. Salinas, S. J. Benkovic, M. J. Natan, C. D. Keating, *J. Am. Chem. Soc.* **2000**, *122*, 9071 – 9077.
[16] a) D. R. Walt, *Science* **2000**, *287*, 451 – 452; b) R. J. Colinas, R. Bellisario, K. A. Pass, *Clin. Chem.* **2000**, *46*, 996 – 998; c) S. Brenner, M. Johnson, J. Bridgham, G. Golda, D. H. Lloyd, D. Johnson, S. Luo, S. McCurdy, M. Foy, M. Ewan, R. Roth, D. George, S. Eletr, G. Albrecht, E. Vermaas, S. R. Williams, K. Moon, T. Burcham, M. Pallas, R. B. DuBridge, J. Kirchner, K. Fearon, J. Mao, K. Corcoran, *Nat. Biotechnol.* **2000**, *18*, 630 – 634; d) J. A. Ferguson, F. J. Steemers, D. R. Walt, *Anal. Chem.* **2000**, *72*, 5618 – 5624.
[17] C. M. Niemeyer, W. Bürger, J. Peplies, *Angew. Chem.* **1998**, *110*, 2391 – 2395; *Angew. Chem. Int. Ed.* **1998**, *37*, 2265 – 2268.
[18] S. Mann, W. Shenton, M. Li, S. Connolly, D. Fitzmaurice, *Adv. Mater.* **2000**, *12*, 147 – 150.
[19] C. M. Niemeyer, B. Ceyhan, S. Gao, L. F. Chi, S. Peschel, U. Simon, *Colloid Polym. Sci.* **2001**, *279*, 68 – 72.
[20] C. M. Niemeyer, M. Adler, D. Blohm, *Anal. Biochem.* **1997**, *246*, 140 – 145.
[21] M. Gottlieb, M. Chavko, *Anal. Biochem.* **1987**, *165*, 33 – 37.

The Unusual Formation of Iron Silicide by Reaction of Iron with $SiCl_4$**

Michael Binnewies,* Arndt Meyer, and Mike Schütte

Dedicated to Professor Hans Georg von Schnering on the occasion of his 70th birthday

A wide variety of metallic compounds, especially borides, carbides, and silicides[1] are attractive materials for technical applications due to their hardness and high melting points. As these compounds often are brittle, their preparation and shaping are particularly demanding tasks. Sintering processes require high temperatures and are thus energy- and time-consuming. Herein, we report on a fast chemical reaction of a metal with a nonmetallic compound, in which a metal silicide is generated that surprisingly retains the original shape of the metal. In this way, it is possible, in principle, to produce a material from a tractable, deformable metal, which possesses the shape of the metal employed.

During a chemical reaction of metals with nonmetals or nonmetallic compounds, the outer shape of the utilized metal is completely altered. Regardless of whether the metal is subjected to the reaction as a powder, sheet, or wire, its original shape is unrecognizable after the reaction and the product is formed as a powder. The aim of our experiments was to develop a method for the preparation of refractory alloys, borides, carbides, and silicides that allows these materials to be obtained in a homogeneous phase-pure form and in a short time. Generally, the synthesis of the above-mentioned species from the elements is very inefficient even at high temperatures because the diffusion coefficients are low; therefore, the reaction often leads to nonhomogeneous products. Our idea was to increase the mobility of both components of the synthesis, metal and nonmetal (B, C, Si), to produce a homogeneous metal – nonmetal compound in a

[*] Prof. Dr. M. Binnewies, Dipl.-Chem. A. Meyer, Dipl.-Chem. M. Schütte
Institut für Anorganische Chemie der Universität Hannover
Callinstrasse 9, 30167 Hannover (Germany)
Fax: (+49) 511-762-19032
E-mail: binn@aca.uni-hannover.de

[**] This work was supported by the Deutsche Forschungsgemeinschaft and the Fonds der Chemischen Industrie. We thank Dr. Köpke, Institut für Mineralogie, Universität Hannover, for the microprobe analyses.

  1433-7851/01/4019-3688 $ 17.50+.50/0